Mon. Not. R. Astron. Soc. **269,** 913–920 (1994)

ROSAT constraints on the intermediate polar candidates V 426 Oph, SW UMa and 1H0709 − 360

S. R. Rosen, K. L. Clayton, J. P. Osborne and P. A. McGale
Department of Physics and Astronomy, University of Leicester, University Road, Leicester LE1 7RH

Accepted 1994 March 16. Received 1993 December 10

ABSTRACT

ROSAT observations of three cataclysmic variables with disputed intermediate polar (DQ Her star) designations are presented. Pronounced variability, with possible timescales of 12.5, 2.5 or 4.5 h, is seen in the X-ray light curve of V426 Oph; these variations may be accompanied by spectral changes. This system may have been caught in the decline from a dwarf nova outburst, being significantly brighter and softer during the early part of the observation. The previously reported orbital and rotational X-ray/optical periodicities in SW UMa were not detected in the *ROSAT* observations of this star: we place an upper limit of 20 per cent on the pulse fraction of any rotational modulation. Spectral analysis indicates that a two-temperature origin for the X-ray emission is probably appropriate. An X-ray imaging detection of the *HEAO-1* source, 1H0709 − 360, is also presented. The weak signal precludes a detailed spectral analysis, but we are able to place limits on the column to the source. When extrapolated to the 2–10 keV band, the constraints imposed by the *ROSAT* data yield a flux that is about two orders of magnitude fainter than that implied by the *HEAO-1* detection. The intermediate polar classification of each of the three sources remains unconfirmed.

Key words: stars: individual: V426 Oph – stars: individual: SW UMa – stars: individual: 1H0709 − 360 – novae, cataclysmic variables – X-rays: stars.

1 INTRODUCTION

The X-ray sources V426 Oph, SW UMa and 1H0709 − 360 are all cataclysmic variables (CVs), i.e. short-period binaries consisting of a cool secondary star transferring material to an accreting white dwarf. All have at one time or another been proposed as members of the intermediate polar (IP) (or DQ Her) subclass (V426 Oph – Szkody 1986; SW UMa – Shafter, Szkody & Thorstensen 1986; 1H0709 − 360 – Tuohy et al. 1990). Members of the IP subgroup contain an asynchronously rotating magnetic white dwarf and, as such, are expected to show an X-ray light curve that is strongly modulated at the white dwarf rotation period. In the case of V426 Oph, an IP classification has been refuted (Hellier et al. 1990), since the 60-min spin period claimed to have been seen in the *EXOSAT* X-ray light curves, which together with the ~6-h optical radial velocity period led to its proposal as an IP (Szkody 1986), was not witnessed in optical radial velocity measurements. A subsequent re-analysis of the *EXOSAT* data on V426 Oph by Hellier et al. (1990) found that the 60-min period was not, in fact, significant.

The IP classification of SW UMa was first proposed by Shafter et al. (1986), based on optical and X-ray observations in quiescence. They found an 81.8-min radial velocity period and a 15.9-min optical photometric variation. The X-ray data showed modulation at both periods. The detection of superhumps by Robinson et al. (1987) showed that SW UMa is also an SU UMa-type system. An *EXOSAT* observation during superoutburst showed no X-ray modulation at either the 81- or 15.9-min periods (Szkody, Osborne & Hassall 1988). The 15.9-min period has not been convincingly detected in subsequent optical observations, either when the system was in an anomalous faint state (Howell & Szkody 1988) or in a superoutburst state (Kato, Hirata & Mineshige 1992).

1H0709 − 360 was discovered by Tuohy et al. (1990) as an eclipsing CV with a binary period of 2.44 h, within the 2–3 h period gap. These authors suggested, on the basis of its strong He II emission, the presence of a hard X-ray flux and the possible existence of a second periodicity close to the orbital period, that 1H0709 − 360 might be an IP close to synchronism.

In the present paper, we present the results of pointed *ROSAT* soft X-ray observations of these CVs.

2 OBSERVATIONS

2.1 V426 Oph

V426 Oph was observed by *ROSAT* over an extended interval of $\sim 10^6$ s, starting on 1991 March 17. Data were recorded with the Position Sensitive Proportional Counter (PSPC) at the focus of the X-ray telescope (XRT) and the EUV Wide-Field-Camera (WFC) (for a description of the *ROSAT* satellite and its instrumentation, see Pfefferman et al. 1986; Wells et al. 1990, and references therein). The total PSPC on-source exposure time of 16.5 ks was divided between 10 windows, each lasting between 20 and 35 min. The first two windows were separated by about a day (15 spacecraft orbits) and preceded, by about 10 days, a run of eight windows during nine contiguous spacecraft orbits. All PSPC observations were performed with the filter wheel in the open position (0.1–2.5 keV), and the source was observed on-axis. The entire WFC on-source exposure of 11 ks was secured through the S1A (65–140 Å: 88–190 eV) filter.

2.2 SW UMa

ROSAT observations of SW UMa were made during two intervals, one on 1992 April 11 and the second on 1992 May 3. Both PSPC observations were acquired with the filter wheel at the open position, and they had a combined exposure time of 6 ks. WFC observations of 2580 and 1040 s were recorded through the S1A and S2B (112–200 Å: 60–110 eV) filters, respectively. The observations were performed with the target on-axis.

2.3 1H0709 − 360

1H0709 − 360 was the target of a short *ROSAT* pointing on 1991 October 4, with a total PSPC exposure of 8 ks during an interval of ~ 7 h. The target was observed on-axis with the filter wheel in the open position.

3 RESULTS

3.1 V426 Oph

3.1.1 The X-ray light curve

An image generated from the PSPC data revealed a bright source at the centre, whose measured coordinates, determined by fitting the known point response function to the profile of the source distribution, lie within 8 arcsec (cf. the attitude uncertainty of about 10 arcsec) of the known optical position of V426 Oph. The source was detected at a mean level of 0.473 ± 0.006 count s^{-1} in the PSPC.

A PSPC light curve of V426 Oph, integrated into 60-s bins, was constructed by summing the counts accumulated within 3.5 arcmin of the source centre and subtracting from this an appropriately scaled background light curve derived from an offset region of radius 6 arcmin, located so as to avoid contaminating sources in the field. The resulting time series, shown in Fig. 1, exhibits marked variability which is manifested in several forms. First, the mean level of the first two windows (0.78 ± 0.02 count s^{-1}) lies well above that (0.38 ± 0.01) of the last eight. Flickering is also evident: prominent examples are visible in the first and seventh windows of the contiguous sequence in Fig. 1. Fourier analysis of the data in the individual windows, binned at 3-s resolution, reveals a variation with a period of 100 s and an amplitude ~ 30 per cent which is present in, and coherent between, the first two windows. However, inspection of an

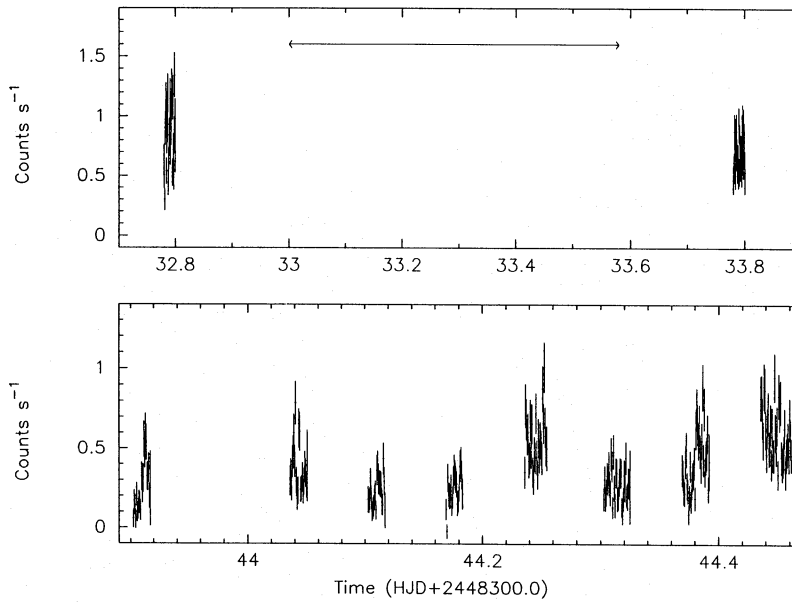

Figure 1. The *ROSAT* PSPC (0.1–2.5 keV) light curve of V426 Oph. The top panel shows the data from the first and second *ROSAT* windows, respectively, whilst the lower panel displays the section of data containing the eight adjacent windows. The bar in the upper panel indicates the entire temporal extent of the lower panel.

image constructed in detector coordinates suggests that this 100-s modulation is associated with the cyclic passage of the source under the detector window support wires on the 400-s wobble period of the satellite.

More intriguing, however, is the distinct, slow pattern of variability seen in the contiguous sequence of eight windows in Fig. 1. The deviations of the data about their mean level in these last eight windows yield a negligible probability that this part of the light curve is constant. After allowing for a linear trend, Fourier and sine-fitting analyses applied to these data (which span about 14 h) suggest three possible time-scales for the apparent 'modulation' – 4.5 ± 0.1, 2.51 ± 0.05 or $\sim 1.25 \pm 0.02$ h: the period ambiguity arises from the sampling of the underlying modulation by the *ROSAT* window pattern. Characterization of the variation in terms of a sine function yields mean semi-amplitudes (about the mean) of 55 ± 11, 48 ± 12 and 42 ± 9 per cent for the 4.5-, 2.5- and 1.25-h time-scales, respectively – uncertainties for both the periods and modulation fractions are 68 per cent (68 per cent uncertainties are used throughout this paper unless otherwise stated), and were derived after scaling the data error bars to normalize the best-fitting reduced chi-squared to 1.0 to allow for flickering. Nevertheless, the data in the last eight windows span only ~ 3 cycles of the apparent ~ 4.5-h variation, and we are thus unable to establish conclusively whether the variability is periodic. In fact, the only other reliable period quoted for V426 Oph is the optical radial velocity period of 6.8 h determined by Hessman (1988), which is currently associated with the orbital period of the system. The three possible variability time-scales noted in our *ROSAT* data are not compatible with the 6.8-h orbital period. The linearly detrended data were also folded on the 60-min period mooted by Szkody (1986). The best-fitting sinusoid gives a fractional amplitude of 15 ± 8 per cent, but is consistent with no modulation within the lower 3σ bound of the amplitude. A 3σ upper limit of 32 per cent can be placed on the semi-amplitude of any 60-min sinusoidal modulation in our *ROSAT* data.

Although V426 Oph was observed with the WFC for 11 ks during the pointed observation, it was not detected. The source was also scanned during the WFC survey (in 1990 September) for a total of ~ 1500 s, but was also undetected then. Despite the much longer pointed exposure, higher sensitivity was actually achieved from the survey, due largely to the $\sim$ six-fold reduction in detector efficiency that resulted from the catastrophic loss of satellite attitude control in 1991 January. We have therefore used the survey data to derive 3σ upper limit count rates of 0.15 and 0.08 count s^{-1} in the S1A and S2B filters, respectively.

3.1.2 *The spectrum*

To test for systematic spectral variability in the *ROSAT* data of V426 Oph, a curve of hardness ratio against time was computed (in 300-s bins), based on the ratio of counts in PSPC channels 111–240 ($\sim$ 1–2.5 keV) to those in channels 8–110 ($\sim$ 0.1–1 keV). The results indicate that the mean ratio of the first two windows (1.10 ± 0.05) differs from that of the last eight (1.41 ± 0.06) with greater than 99 per cent confidence. However, there were no obvious signs of systematic variability on time-scales < 14 h (the span of the eight contiguous windows). Consequently, we initially accumulated two spectra, one averaged over the first two windows and the other over the last eight.

Both spectra were compared against blackbody, power-law and thermal-bremsstrahlung emission models, each model providing a formally acceptable fit to both datasets. The results are presented in Table 1. The thermal-bremsstrahlung model is consistent with the spectrum of the last eight windows for temperatures > 7.5 keV (99 per cent confidence limit) – the PSPC cannot reliably determine temperatures greater than a few keV. A Raymond & Smith plasma model was also fitted to the spectrum of the first two windows, since the fitted bremsstrahlung temperature of 2.4 keV suggests that contributions from emission lines may be significant. This resulted in a temperature of $4.6^{+3.6}_{-1.5}$ keV, a column of $2.1^{+0.4}_{-0.2} \times 10^{21}$ cm^{-2} ($\chi^2 = 26.0$, $\nu = 30$ – the abundances were fixed at 1.0 relative to solar) and an integrated flux of 9.4×10^{-12} erg s^{-1} cm^{-2} in the 0.1–2.5 keV band. In accord with the import of the hardness-ratio change, the principal conclusion of this spectral analysis is that the spectrum shows a distinct hardening in the last eight windows of the observation. This is illustrated graphically in Fig. 2, where we show, for the two data sections, various confidence contours in the α–N_H plane of the power-law model.

In comparing our *ROSAT* spectra with the results obtained from the *EXOSAT* analysis (Szkody 1986), it became apparent that the inclusion of an iron feature in the

Table 1. Spectral parameters of V426 Oph for the best-fitting blackbody, power-law and thermal bremsstrahlung emission models derived from the spectra of the first two windows of data and for the last eight. Each fit has 30 degrees of freedom. Uncertainties are based on two parameters of interest and are the 90 per cent confidence values.

Blackbody model

Windows	$N_H \times 10^{21}$ (cm^{-2})	kT (keV)	χ^2	Flux (0.1-2.5 keV) (ergs s^{-1} cm^{-2})
1-2	$0.95^{+0.90}_{-0.52}$	0.42±0.07	29.3	8.8×10^{-12}
3-10	$0.56^{+0.56}_{-0.29}$	0.72±0.13	31.9	5.8×10^{-12}

Power law model

Windows	$N_H \times 10^{21}$ (cm^{-2})	α	χ^2	Flux (0.1-2.5 keV) (ergs s^{-1} cm^{-2})
1-2	$3.4^{+1.6}_{-1.4}$	2.1±0.8	24.9	9.1×10^{-12}
3-10	$1.6^{+1.1}_{-0.8}$	$0.56^{+0.50}_{-0.41}$	27.2	6.0×10^{-12}

Bremsstrahlung model

Windows	$N_H \times 10^{21}$ (cm^{-2})	kT (keV)	χ^2	Flux (0.1-2.5 keV) (ergs s^{-1} cm^{-2})
1-2	$2.7^{+1.1}_{-0.9}$	$2.4^{+12.9}_{-1.2}$	25.7	9.1×10^{-12}
3-10	2.9±0.4	195_{-160}	34.3	5.6×10^{-12}

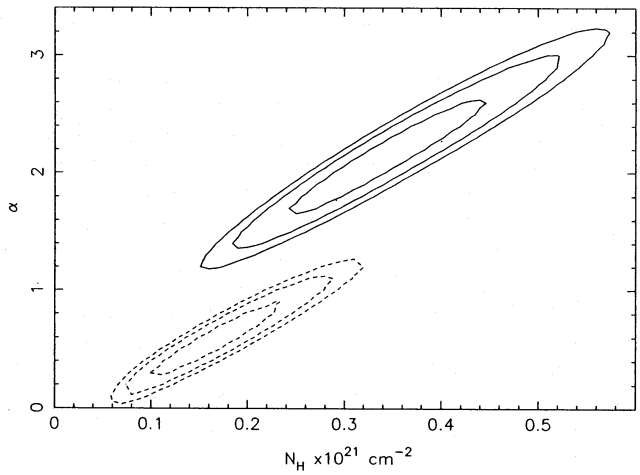

Figure 2. The 68 (inner), 95 and 99 per cent (outer) confidence contours in the photon index–column density plane for power-law model fits to the spectra of V426 Oph. The solid contours are for the spectrum representing windows 1 and 2, whilst the dashed contours delineate the parameter ranges of the spectrum averaged over the last eight windows.

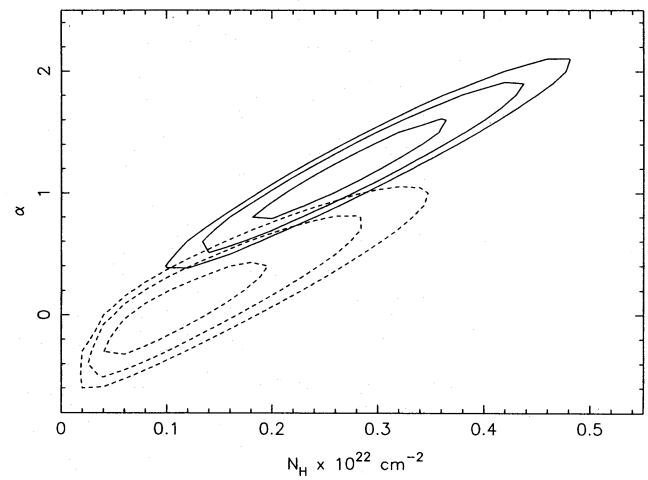

Figure 3. As for Fig. 2, but for spectra centred on the bright (solid) and faint (dashed) intervals of the apparent modulation during the last eight windows.

fits to the *EXOSAT* data might be appropriate. We therefore re-extracted the *EXOSAT* spectrum from the *EXOSAT* archive and tested several emission models against the data. Fits to the combined *EXOSAT* ME and LE data are improved with 94 per cent confidence if an iron feature is added to the thermal-bremsstrahlung model. The best-fitting parameters are $kT = 18.8^{+10.7}_{-5.3}$ keV, $N_H = 4.1^{+1.6}_{-0.9} \times 10^{21}$ cm^{-2}, an iron-line centroid energy of ≈ 6.8 keV and equivalent width of 0.67 keV, yielding $\chi^2 = 18.0$ for 23 degrees of freedom. When applied to the mean *ROSAT* spectrum of V426 Oph from the last eight windows, a thermal-bremsstrahlung model with the temperature and column fixed at these values results in an unacceptable fit ($\chi^2 = 61.8$ for 32 degrees of freedom). However, the uncertainties on the parameters derived from the *ROSAT* and *EXOSAT* data overlap at about the 5 per cent confidence level. There is a negligible probability that the *EXOSAT* results are consistent with those pertaining to the spectrum of the first two *ROSAT* windows.

To test more sensitively for spectral variability amongst the last eight windows, we produced a curve of hardness ratio against flux using the 60-s time-bins from these windows. The slope of the best-fitting linear function is inconsistent with zero at better than 99 per cent confidence. As a result, we also generated two spectra which separately covered the bright and faint halves of the approximately 4.5-h variation seen in the last eight windows. Power-law models were fitted to each spectrum, yielding $\alpha = 1.2 \pm 0.5$, $N_H = 2.7 \pm 1.0 \times 10^{21}$ cm^{-2} ($\chi^2 = 25.4$, $\nu = 30$) for the bright interval and $\alpha = -0.02^{+0.47}_{-0.33}$, $N_H = 0.9^{+1.1}_{-0.5} \times 10^{21}$ cm^{-2} ($\chi^2 = 32.9$, $\nu = 30$) for the faint portion. Confidence contours in the α–N_H plane are shown in Fig. 3. These results show that the spectra from the faint and bright periods differ with > 99 per cent confidence, and that, during the decline into the faint interval, the predominant spectral change is a hardening of the flux, although it may also be accompanied by a decrease in the absorbing column.

3.2 SW UMa

3.2.1 The X-ray light curve

SW UMa was detected at a mean count rate of 0.35 count s^{-1} in the PSPC. The light curve was extracted in a manner similar to that employed for V426 Oph, again using an offset background region but with 30-s bins. Although the light curve (Fig. 4) of SW UMa shows no obvious systematic variability within either data section, the target was 27 per cent brighter on April 11 than on May 3. SW UMa was not detected by the WFC in either the pointed observations or the survey. Upper limits (3σ) based on the WFC survey scans are 0.020 count s^{-1} (2120-s exposure) and 0.021 count s^{-1} (1830-s exposure) in the S1A and S2B filters, respectively. An optical light curve provided by the AAVSO (J. Mattei 1993, private communication) is shown in Fig. 5 and indicates that SW UMa was observed in its quiescent state by *ROSAT*, the X-ray observation beginning about 4 d after the end of the previous outburst.

The PSPC data were examined using both Fourier and folding techniques. A Fourier analysis, restricted to periods between 30 and 2000 s, found no significant power in this range, with a 3σ upper limit on the semi-amplitude of 21 per cent. The accuracy of the 15.9-min period (assuming an uncertainty of ± 0.1 min) reported by Shafter et al. (1986) is insufficient, over the 19-d separation of the two *ROSAT* observations, to generate a folded light curve of the combined data. We therefore treated each observation separately, subtracting a low-order polynomial from the data and folding the residuals on a period of 15.9 min. The tighter measurement yields a 95 per cent upper limit of 20 per cent on the semi-amplitude of any 15.9-min modulation. We emphasize, however, that neither *ROSAT* observation spans more than three cycles of this time-scale. Although neither *ROSAT* observation alone samples more than about 60 per cent of the 81-min orbital period, we tested for its presence by fitting an orbital sinusoid to each section separately. No such modulation was detected with a 95 per cent upper limit of 58 per cent on the fractional semi-amplitude about the mean.

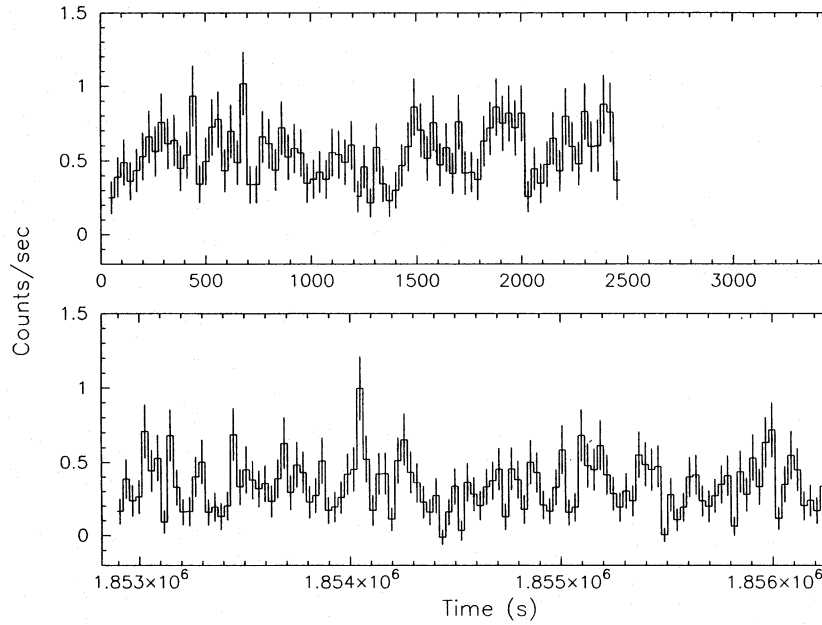

Figure 4. The *ROSAT* PSPC light curvevs of SW UMa. The upper panel shows the data taken on 1992 April 11, whilst the data from 1992 May 3 are displayed in the lower panel.

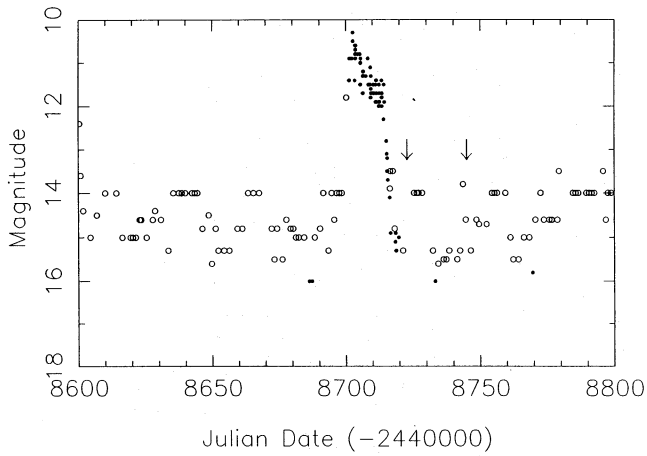

Figure 5. The AAVSO light curve of SW UMa spanning an interval of 200 d around the time of the *ROSAT* observation. The open circles indicate upper limits. Arrows mark the epochs of the *ROSAT* observations.

3.2.2 *The spectrum*

A search for spectral variations in the SW UMa PSPC data was conducted by computing a time-resolved curve of the hardness ratio, using the ratio of pulse-height channels 11–30/31–200 (i.e. 0.1–0.3 keV/0.3–2 keV) in 60-s bins. Tests of the data, with various binning factors, against the hypothesis of constancy revealed no significant variation on time-scales greater than 60 s. As a result, spectral fits were made to the time-averaged spectrum, using blackbody, bremsstrahlung, power-law and Raymond & Smith models. The results are displayed in Table 2. Simple models do not fit the data. Two-component models provided a better match. A two-component, Raymond & Smith model with tempera-

Table 2. Spectral parameters for the best-fitting power-law, bremsstrahlung, and single- and two-temperature Raymond & Smith models applied to the *ROSAT* data of SW UMa. Uncertainties are based on two parameters of interest, and are 90 per cent confidence values. Uncertainty ranges were not assigned for the parameters of the power-law model or the single-component Raymond & Smith model, because the fits are statistically unacceptable.

Power law model

$N_H \times 10^{19}$ (cm^{-2})	α	χ^2, ν	Flux (0.1-2.5 keV) (ergs s^{-1} cm^{-2})
9.1	1.8	56.7, 29	2.9×10^{-12}

Bremsstrahlung model

$N_H \times 10^{19}$ (cm^{-2})	kT (keV)	χ^2, ν	Flux (0.1-2.5 keV) (ergs s^{-1} cm^{-2})
$5.7^{+2.8}_{-2.4}$	$1.7^{+0.8}_{-0.4}$	44.9, 29	2.8×10^{-12}

Raymond-Smith model

$N_H \times 10^{19}$ (cm^{-2})	kT (keV)	χ^2, ν	Flux (0.1-2.5 keV) (ergs s^{-1} cm^{-2})
0.6	2.69	66.85, 29	2.8×10^{-12}

Two Temperature Raymond Smith model

$N_H \times 10^{19}$ (cm^{-2})	kT_1 (keV)	kT_2 (keV)	χ^2, ν	Flux (0.1-2.5 keV) (ergs s^{-1} cm^{-2})
$0.4^{+2.3}_{-0.4}$	$0.37^{+0.27}_{-0.17}$	$2.8^{+5.9}_{-1.6}$	35.36, 27	2.7×10^{-12}

tures of $0.37^{+0.27}_{-0.17}$ keV and $2.8^{+5.9}_{-1.6}$ keV and a common absorbing column, N_H, of $0.4^{+2.3}_{-0.4} \times 10^{19}$ atom cm^{-2} yielded the best fit, although other two-component models, e.g. blackbody plus bremsstrahlung, also provided acceptable results ($\chi^2 = 37.3$, $\nu = 28$). Confidence limits on the temperature and column parameters of the two-component, Raymond & Smith model are presented graphically in Fig. 6. The implied 2–6 keV band (absorbed) fluxes of the low-and high-temperature components are 1.7×10^{-15} and 1.1×10^{-12} erg s^{-1} cm^{-2}, respectively.

3.3 1H0709 − 360

X-ray emission from a point source, whose centroid is located within 12 arcsec of the reported optical position of 1H0709 − 360, was detected at a mean count rate of 0.003 ± 0.001 count s^{-1} (4.1σ detection) in the *ROSAT* PSPC field. This *ROSAT* observation represents the first X-ray imaging detection of the X-ray counterpart to the optical CV. The source was not detected in the WFC in either the pointed or survey observations. The survey data provide 3σ upper limits of 0.01 count s^{-1} in both the S1A and S2B filters, based on exposure times of ~2400 and ~2050 s, respectively.

The PSPC light curve of 1H0709 − 360 was binned into 100-s bins. Whilst we find no significant evidence of systematic variability in the light curve when folded on the 2.444-h orbital period identified by Tuohy et al. (1990), the poor statistical quality of the data permits a 100 per cent modulation within the 95 per cent confidence level.

The low PSPC count rate measured for 1H0709 − 360 precludes a detailed spectral investigation. Nevertheless, we are able to place constraints on the spectral parameters of the source by forming an average hardness ratio from the counts measured in pulse-height channels 41–200 (0.4–2 keV) and 8–40 (0.1–0.4 keV) and then comparing the resulting ratio, 5.79 ± 7.34, with the values expected for a Raymond & Smith plasma model, evaluated over a grid of points in the kT–N_H plane. Fig. 7 shows the allowed regions of parameter space. While the temperature is essentially unconstrained, at the 95 per cent level, the column density is less than 10^{21} cm^{-2}, unless the temperature is below about 0.4 keV. For temperatures above 1 keV, the column density is less than 7×10^{20} cm^{-2}, with 95 per cent confidence. Assuming the temperature to lie in the range 0.1–30 keV, we estimate an upper limit for the observed flux at Earth of 1×10^{-13} erg s^{-1} cm^{-2} in the 0.1–2.5 keV band and, by extrapolation, a corresponding 2–10 keV flux of 2.8×10^{-13} erg s^{-1} cm^{-2}.

4 DISCUSSION

4.1 V426 Oph

Our analysis of the *ROSAT* PSPC data from V426 Oph has revealed tentative evidence for variability with a time-scale of 1.25, 2.5 or 4.5 h, during an interval of about 14 h. However, whether this variability is strictly periodic or simply reflects short (~hour) time-scale fluctuations is untestable in the current data, due both to the gaps in the time series arising from the satellite sampling pattern and to the brevity of the observation relative to the longest of the possible 'periods'. Even if confirmed, none of these most probable time-scales allowed by the *ROSAT* data is consistent with the known 6.8-h binary period of V426 Oph (Hessman 1988). Whilst the shortest (1.25-h) 'period' is comparable to the 1-h modulation claimed by Szkody (1986) (but dismissed by Hellier et al. 1990), it is not consistent with that period: an *F*-test shows that the 1.25-h modulation time-scale is preferred at the 98 per cent level over a 1-h variation in the *ROSAT* data. Conversely, there is no evidence of a counterpart to the 1.25-h *ROSAT* 'time-scale' in the *EXOSAT* data. Nevertheless, comparison of the spectra from the bright and faint portions of the *ROSAT* variation does suggest that it may be accompanied by spectral changes in which the source hardens during the trough of the cycle. It is interesting to note that the spectral changes are primarily confined to the spectral slope. Amongst the known IPs, an increase in absorbing column during the rotational minimum is a

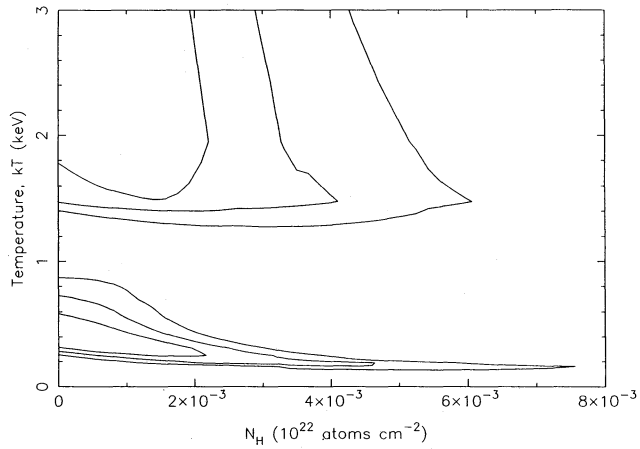

Figure 6. 68 (innermost), 95 and 99 per cent (outermost) confidence contours for the parameters of the two-component, Raymond & Smith plasma model applied to the *ROSAT* spectrum of SW UMa.

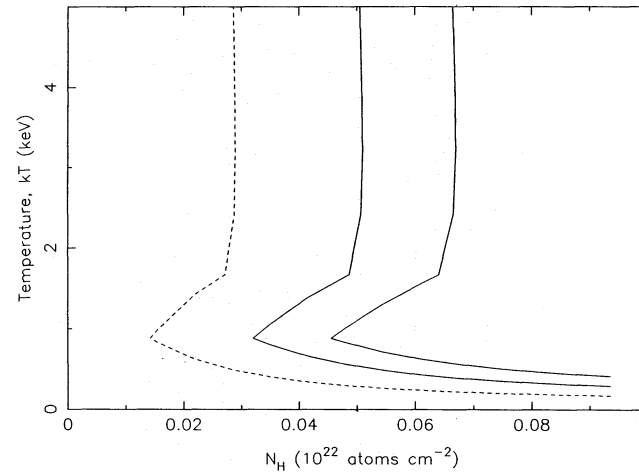

Figure 7. Contours of the measured hardness ratio (dashed line) and its 68 (leftmost solid line) and 95 per cent (rightmost solid line) confidence limits for 1H0709 − 360 are mapped on a grid of such values in the kT–N_H plane for a Raymond & Smith emission model.

ubiquitous property (e.g. Norton & Watson 1989). However, in V426 Oph, if anything, the column shows a *decrease* towards flux minimum, suggesting that, if V426 Oph were an IP, the variation witnessed in the *ROSAT* data is unlikely to be due to rotational effects. Further X-ray observations of V426 Oph over an extended baseline will be needed to resolve the issue of periodic X-ray variability in this star.

The long-term flux and spectral changes that occur between the mean spectrum of the first two windows of the *ROSAT* observation and that of the last eight are highly significant. The behaviour of the bolometric X-ray flux, if mimicked in the optical band, would correspond to a brightness change of about 0.8 mag, suggesting that the source may have been in outburst during the first two windows. Optical data, supplied to us by the AAVSO (J. Mattei 1993, private communication), are displayed in Fig. 8, and show that the star was certainly at its quiescent level of about magnitude 13 during the latter part of the *ROSAT* observation. However, a gap of about 100 d is present in the AAVSO light curve (due to the source disappearing into the day sky). This interval extends just beyond the epochs of the first two *ROSAT* windows, so we are unable to establish its optical state at that time. The suggestion that the star may have been in outburst during the early part of the *ROSAT* observation is not unreasonable. Outbursts of 1–2 mag are known to occur in V426 Oph with intervals of typically 20–50 d, a time-scale confirmed by the appearance of several such events in the AAVSO data. The first outburst subsequent to our observations occurred about 34 d after the first two *ROSAT* windows. The softening of the source during the first two *ROSAT* windows also points to the system being in outburst – such a phenomenon is expected (e.g. Pringle & Savonije 1979) if the emission arises from a simple boundary layer. Indeed, dwarf novae characteristically show a dramatic softening of their X-ray emission during outburst. However, in outbursting dwarf novae for which good-quality soft X-ray data exist, the blackbody temperature that characterizes the soft component is typically much lower, ~10 eV (e.g. SS Cyg, Córdova et al. 1980; VW Hyi, Van der Woerd & Heise 1987; U Gem, Córdova et al. 1984), than the temperature (~0.4 keV) measured during the suspected outburst observed in our *ROSAT* data of V426 Oph. Since outbursts in V426 Oph can last for several days, it may be that *ROSAT* caught the system at a point well into the decline phase of a more luminous (2–3 mag) outburst, with the spectrum being increasingly dominated by optically thin emission as it returned to the quiescent level. The accretion rate is also an important factor. The putative boundary layer is thought to be optically thin during quiescence, but to become optically thick during outburst. In V426 Oph, the change in accretion rate that gives rise to the outburst is perhaps only a factor of ~3, as indicated by the generally low flux amplitudes of the outbursts. Since the optical depth is a function of accretion rate, it may be that the emission region does not become completely optically thick, but continues to radiate a substantial hard bremsstrahlung component. Nevertheless, in the absence of more comprehensive coverage of an outburst in this star, these hypotheses remain speculative.

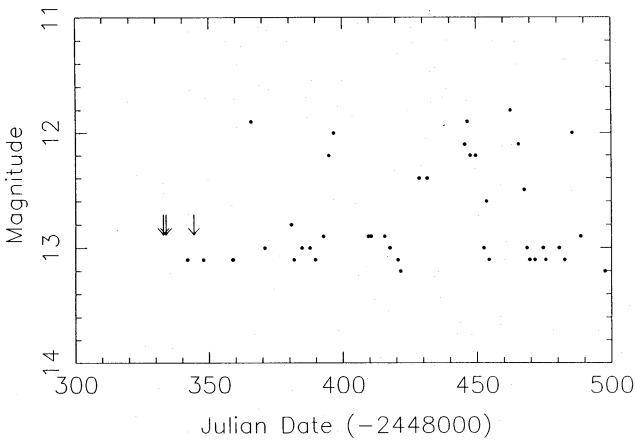

Figure 8. AAVSO optical light curve of V426 Oph spanning the interval of the *ROSAT* observations. A break of about 100 d in the coverage, when the star passed into the day sky, overlaps the first two *ROSAT* windows. Several outbursts are seen in the subsequent period. The star is at its quiescent level during the last eight *ROSAT* windows. Arrows mark the epochs of the *ROSAT* observations – the rightmost arrow indicates the mid-point of the eight-window sequence.

4.2 SW UMa

The *ROSAT* PSPC observations of SW UMa show no convincing evidence of the 15.9-min modulation that was witnessed in the *EXOSAT* ME (1–8 keV) data of the source taken during quiescence (Shafter et al. 1986). Our 2σ upper limit of 20 per cent on the modulation semi-amplitude, however, is consistent with the 28 ± 17 per cent semi-amplitude observed in the *EXOSAT* data. As such, our data do not exclude the presence of the suggested 15.9-min period.

Based on an *F*-test, the spectral profile measured from the PSPC data indicates that a two-temperature representation is preferred with about 90 per cent confidence over one-component models. It is interesting to note that the temperatures (0.37 and 2.8 keV) measured for SW UMa in these data are comparable to those (0.7 and 9 keV) derived for the IP, EX Hya (Singh & Swank 1993). Two-component models that have been applied in non-magnetic dwarf novae such as SS Cyg indicate a much lower temperature, blackbody source (e.g. Jones & Watson 1992, and references therein) for the cool component.

4.3 1H0709 − 360

We have obtained the first X-ray imaging detection of the X-ray counterpart to the optical CV that was associated with the *HEAO-1* X-ray source, 1H0709 − 360. The source is, however, only detected weakly by *ROSAT*, and we are unable to confirm or reject the presence of an orbital modulation. The spectrum is also poorly constrained, but the intervening absorbing column density is likely to be less than 10^{21} cm^{-2}. Within the constraints imposed by the *ROSAT* data, the predicted flux in the 2–10 keV band of 2.8×10^{-13} erg s^{-1} cm^{-2} indicates that the point source in the *ROSAT* image is a factor $\gtrsim 70$ fainter than the source of emission detected by *HEAO-1* (Tuohy et al. 1990). We find no X-ray objects visible within the *ROSAT* field that lie within both the *HEAO-1* MC and LASS error boxes (see Tuohy et al. 1990), and that could explain this large flux discrepancy. There are three possible explanations. The target,

1H0709−360, may be highly variable, perhaps having been in outburst during the *HEAO-1* observation. In the context of the IPs, whilst four of the group are known to exhibit outburst behaviour (EX Hya – e.g. Hellier et al. 1989; V1223 Sgr – van Amerongen & van Paradijs 1989; TV Col – Szkody & Mateo 1984; GK Per – e.g. King, Ricketts & Warwick 1979), only in the last case have X-ray observations been secured in both outburst and quiescent states (Watson, King & Osborne 1985; Ishida et al. 1992). The implied flux change in 1H0709−360 would be significantly larger than anything witnessed in GK Per during its outbursts. An alternative scenario is that the *HEAO-1* flux is dominated by one or more sources that are not intrinsically luminous in the 0.1–2.5 keV band and/or are heavily absorbed, explaining the lack of a prominent candidate in the *ROSAT* field. The third possibility is that the spectrum of 1H0709−360 is, in fact, composed of two components, one hard and one soft, with the *ROSAT* data being dominated by the soft component. If the hard component contributes only weakly in the 0.1–2.5 keV band, the poor statistical quality of the data means we would be unable to detect it, leading to a substantial underestimate of the 2–10 keV flux based on an extrapolation of the soft-component spectrum. However, a hard bremsstrahlung or power-law component would have to be heavily absorbed in comparison to the soft component if it were not to dominate the observed 0.1–2.5 keV band flux. For example, a hard bremsstrahlung source with a temperature ~30 keV that can account for the *HEAO-1* flux but contribute only a fraction of the total 0.4–2.0 keV band PSPC count rate requires $N_{\rm H} \gtrsim 5 \times 10^{22}$ cm^{-2}. Higher column densities are required if the temperature is lower.

5 CONCLUSIONS

We have presented the results of *ROSAT* pointed observations of the three cataclysmic variables V426 Oph, SW UM and 1H0709−360, all of which have been advanced as IP candidates. In V426 Oph, we find that the system was a factor of 2 brighter in X-rays at the start of the observation than at the end, suggesting that it may have been in outburst. This behaviour was accompanied by a distinct hardening of the spectrum during the latter part of the observation when the source is definitely in quiescence. During the last 14 h of the pointing, the source shows marked variability with a time-scale of 1.25, 2.5 or 4.5 h. These time-scales are not consistent with the known 6.8-h orbital period. The previously suggested X-ray period of 60 min is also disfavoured by the *ROSAT* data.

ROSAT observations of SW UMa in its quiescent state show no significant evidence of the 15.9-min period previously witnessed in the quiescent-state *EXOSAT* data of the star, although a modulation at a level similar to that reported from the *EXOSAT* observations is consistent with the *ROSAT* data. The *ROSAT* data show no sign of the 81-min orbital variation also previously reported in the *EXOSAT* X-ray observation. The X-ray spectrum is best characterized by a two-temperature thermal model.

We also report the first imaging detection of the X-ray source 1H0709−360. The signal is, however, very weak, and we are unable to place constraints on any variability. Spectral information is limited, but indicates a column density of less than 10^{21} cm^{-2}. The source flux is too faint, by about two orders of magnitude, to be consistent with the flux detected by *HEAO-1*. Possible explanations include: (1) that the CV has changed in luminosity by a level previously unwitnessed in established IPs, (2) that the *HEAO-1* signal was contaminated by emission from either an intrinsically hard source and/or one that is heavily absorbed, or (3) that 1H0709−360 possesses a two-component spectrum, the hard component of which accounts for the *HEAO-1* flux but is heavily absorbed at lower energies, leaving a softer component to dominate the PSPC band.

In summary, the *ROSAT* observations of V426 Oph, SW UMa and 1H0709−360 do not provide any conclusive evidence in favour of the IP classification of these sources. Continuous, extended X-ray observations of each target will be required to classify these systems unambiguously.

ACKNOWLEDGMENTS

We are grateful to Janet Mattei and the observers of the AAVSO for providing the optical light curves of V426 Oph and SW UMa. KLC acknowledges the support of an SERC studentship.

REFERENCES

Córdova F. A., Chester T. J., Tuohy I. R., Garmire G. P., 1980, ApJ, 235, 163
Córdova F. A., Chester T. J., Mason K. O., Kahn S. M., Garmire G. P., 1984, ApJ, 278, 739
Hellier C., Mason K. O., Smale A. P., Corbet R. H. D., O'Donoghue D., Barrett P. E., Warner B., 1989, MNRAS, 238, 1107
Hellier C., O'Donoghue D., Buckley D., Norton A. J., 1990, MNRAS, 242, 32P
Hessman F. V., 1988, A&A, 72, 515
Howell S. B., Szkody P., 1988, PASP, 100, 224
Ishida M., Sakao T., Makishima K., Ohashi T., Watson M. G., Norton A. J., 1992, MNRAS, 254, 647
Jones M. H., Watson M. G., 1992, MNRAS, 257, 633
Kato T., Hirata R., Mineshige S., 1992, PASJ, 44, L215
King A. R., Ricketts M. J., Warwick R. S., 1979, MNRAS, 187, 77P
Norton A. J., Watson M. G., 1989, MNRAS, 237, 853
Pfefferman E. et al., 1986, Proc. SPIE, 733, 519
Pringle J. E., Savonije G. J., 1979, MNRAS, 187, 777
Robinson E. L., Shafter A. W., Hill J. A., Wood M. A., Mattei J. A., 1987, ApJ, 313, 772
Shafter A. W., Szkody P., Thorstensen J. R., 1986, ApJ, 308, 765
Singh J., Swank J., 1993, MNRAS, 262, 1000
Szkody P., 1986, ApJ, 301, L29
Szkody P., Mateo M., 1984, ApJ, 280, 729
Szkody P., Osborne J. P., Hassall B. J. M., 1988, ApJ, 328, 243
Tuohy I. R., Remillard R. A., Brissenden R. J. V., Bradt H. V., 1990, ApJ, 359, 204
van Amerongen S., van Paradijs J., 1989, A&A, 219, 195
van der Woerd H., Heise J., 1987, MNRAS, 225, 141
Watson M. G., King A. R., Osborne J. P., 1985, MNRAS, 212, 917
Wells A. A. et al., 1990, Proc. SPIE, 1344, 230